Thin Films

Deutsche Ausgabe: DOI: 10.1002/ange.201510291
Internationale Ausgabe: DOI: 10.1002/anie.201510291

Superspreading on Immersed Gel Surfaces for the Confined Synthesis of Thin Polymer Films

Pengchao Zhang, Feilong Zhang, Chuangqi Zhao, Shutao Wang, Mingjie Liu, and Lei Jiang**

Abstract: *Liquid spreading is of significant interest in science and technology. Although surface topography engineering and liquid surface-tension regulating can facilitate spreading, the spreading layers in these strategies are inevitably inhomogeneous or contaminated with surfactants. Herein, we show a general strategy to realize the superspreading of liquids on mutually soluble gel surfaces. The cooperation of the hydraulic pressure under liquid phase and liquid-like property of gel surfaces can dramatically eliminate the local pinning effect and enhance the advancement of three-phase contact line, thus forming stable and homogeneous superspreading liquid layers. Such liquid layers can be converted into various functional thin polymer films with controlled thicknesses (nm- to μm-scale) through one-step polymerization of the reactants. Our strategy offers opportunities for large-scale synthesis of versatile functional thin films for various applications.*

Liquid spreading is of significance in both fundamental wetting research and industrial applications.[1] To realize complete liquid spreading, engineered surface topographies,[2] regulated liquid surface tension,[3] and external forces[4] have been utilized to conquer the pinning effect of three-phase contact line (TCL) to form a liquid layer. In these strategies, however, the spreading layers are typically inhomogeneous, or introduce external contaminants such as surfactants. Therefore, the rapid and complete spreading (defined as superspreading) of liquids remains a highly attractive challenge. Herein, we report a general strategy to realize the superspreading of liquids on mutually soluble gel surfaces in a liquid/liquid/gel tri-phase system, which can achieve a stable and homogeneous liquid layer. The hydraulic pressure generated by the liquid phase, and the liquid-like properties of the gel surfaces, can dramatically eliminate local pinning and enhance the advancement of TCL. It is worth noting that the superspreading of highly viscous liquids can even be realized in this strategy, benefiting from the hydraulic pressure. Furthermore, by introducing the reactants into the superspreading layers of liquids, we can fabricate various functional thin polymer films with controlled thicknesses (nm- to μm-scale) through one-step polymerization. These films could have promising applications in photovoltaic devices, flexible electronics, and separation films.[5]

For complete liquid spreading on solid surfaces, it is generally accepted that there is a precursor film propagating in front of the spreading liquid. Such a precursor film actually leads the liquid spreading.[6] However, the local pinning effect induced by defects or impurities on the solid surfaces can hinder the formation of the precursor film, and consequently limit the infinite spreading of liquids.[2c,7] In contrast to solid surfaces, gels are composed of a liquid phase entrapped in a three-dimensional (3D) crosslinked polymer network through weak interactions (for example, hydrogen bonds, van der Waals forces, or hydrophobic interactions). Accordingly, gels can be considered a quasi-liquid phase, while behaving like a solid.[8] Compared with solid surfaces, the entrapped liquid on the gel surfaces may act as precursor film, potentially leading to complete spreading of the liquids. However, water droplets could not completely spread on hydrogel surfaces in air, which might be attributed to the reorientation of the hydrophobic polymer main chains towards the air.[9] The contact angles (CAs) of water on Ca-alginate, poly(acrylic acid) (PAA), poly(vinyl alcohol) (PVA), and polyacrylamide (PAAm) hydrogel surfaces in air are $5.1 \pm 1.1°$, $8.9 \pm 1.2°$, $10.1 \pm 1.3°$, and $10.8 \pm 1.7°$, respectively (Figure S1). Even after 10 min, the water droplets had not completely spread, nor were they absorbed by the hydrogels (Figure 1 a,b). However, under oil, we could realize the rapid and complete spreading (superspreading) of water droplets on hydrogel surfaces (Figure 1 a,c). Taking PAAm hydrogel as an example, the water CA decreased from 11.0° to 8.8° when the hydrogel was immersed into silicone oil (depth: 1 cm; Figure 1 d). Here, we defined the depth (h) as the distance from the air/liquid interfaces to the top surfaces of spreading liquids (Figure 1 c). By increasing the oil depth, the water CA gradually decreased and became 0° at a depth of 34 cm (Figure 1 d).

The superspreading process of liquids on gel surfaces in a liquid/liquid/gel system was recorded using a high-speed camera. Upon contacting the hydrogel surface, the spherical water droplet immediately split and started to spread on the

[*] Dr. P. Zhang, Dr. C. Zhao, Prof. M. Liu, Prof. L. Jiang
Key Laboratory of Bio-Inspired Smart Interfacial Science and Technology of Ministry of Education
School of Chemistry and Environment
International Research Institute for Multidisciplinary Science
Beihang University
Beijing, 100191 (P.R. China)
E-mail: liumj@buaa.edu.cn
jianglei@iccas.ac.cn
Dr. P. Zhang, Dr. F. Zhang, Prof. L. Jiang
Beijing National Laboratory for Molecular Sciences (BNLMS)
Key Laboratory of Organic Solids
Institute of Chemistry, Chinese Academy of Sciences
Beijing, 100190 (P.R. China)
Dr. P. Zhang, Prof. S. Wang, Prof. L. Jiang
Laboratory of Bio-inspired Smart Interface Science
Technical Institute of Physics and Chemistry
Chinese Academy of Science
Beijing, 100190 (P.R. China)

Supporting information for this article can be found under http://dx.doi.org/10.1002/anie.201510291.

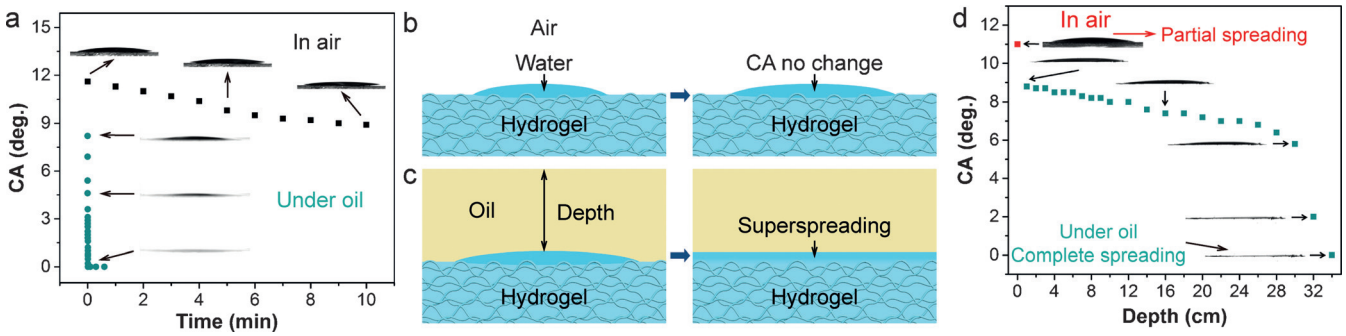

Figure 1. Hydraulic pressure induces complete spreading of water droplets on hydrogel surfaces in an oil/water/hydrogel tri-phase system. a) Time-dependent water CA changes on hydrogel surfaces in air (ambient temperature: 25 °C, humidity: 42 %) and under oil. In air, even 10 min later, the water droplets deposited on PAAm hydrogel surfaces neither completely spread nor adsorbed by the hydrogels. Under oil, water droplets rapidly and completely spread on hydrogel surfaces within 1 s. The CA decrease might be caused by the evaporation of water in air. Illustration of water droplets change b) in air and c) under oil. d) The changes of water CAs with increasing the oil depth.

hydrogel surface (Figure 2a). Then, the whole droplet was rapidly pulled towards the hydrogel surface and achieved complete spreading within 2 s. Similarly, when a poly(butyl methacrylate-*co*-lauryl methacrylate) (P(BMA-*co*-LMA)) organogel,[10] fully swollen by chloroform, was immersed in water, a mutually soluble chloroform droplet exhibited superspreading behavior on its surface (Figure 2b).

The introduction of a liquid phase can significantly increase the spreading coefficient S (Figure 2d,e), which is generally used to predict the liquid spreading on material surfaces.[1,11] Using the spreading of water droplets on hydrogel surfaces as an example, in air (Figure 2c), S can be expressed as:

$$S = \gamma_{ha} - (\gamma_{wa} + \gamma_{hw}) \quad (1)$$

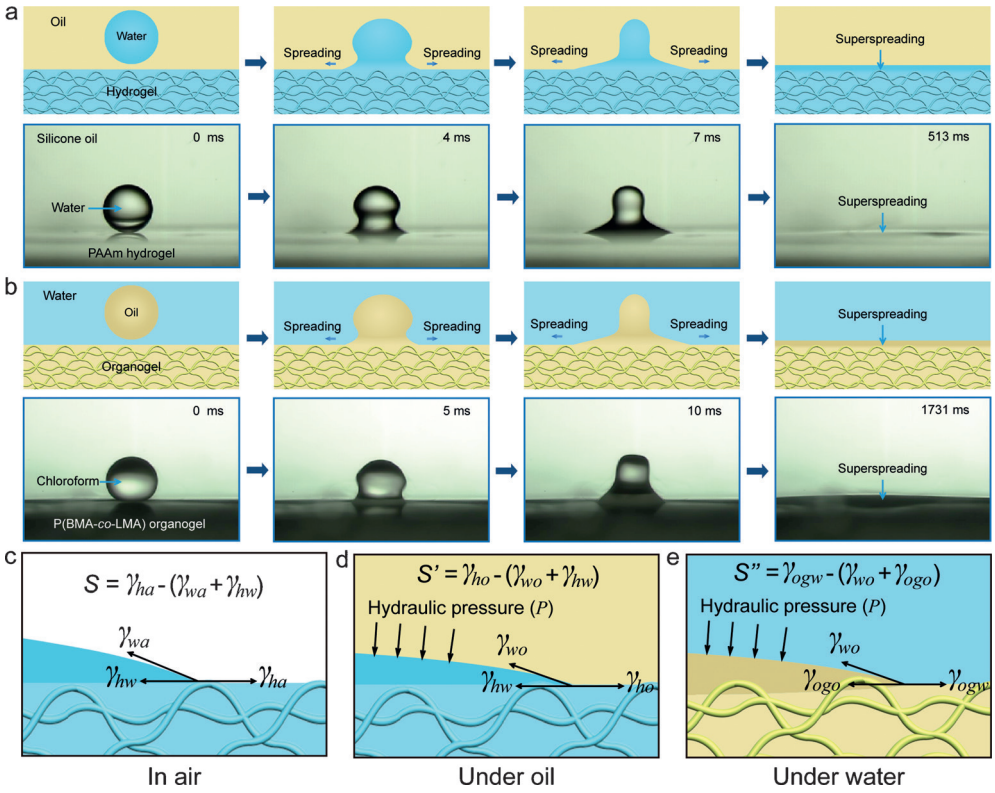

Figure 2. Spontaneous liquid superspreading on gel surfaces in a liquid/liquid/gel tri-phase system. a) Illustration and images of the superspreading processes of a water droplet (5 μL) achieves on PAAm hydrogel surfaces. b) Illustration and images of the superspreading processes of a chloroform droplet (5 μL) rapidly and completely spreading and forming an oil layer on the chloroform-swollen P(BMA-*co*-LMA) organogel surface. Illustrations of the spreading coefficient S of liquid droplets spreading on gels c) in air, d) under oil, and e) under water.

where γ_{ha}, γ_{wa}, and γ_{hw} are the hydrogel/air, water/air, and hydrogel/water interfacial tensions, respectively. While under oil (Figure 2d), S' can be expressed as:

$$S' = \gamma_{ho} - (\gamma_{wo} + \gamma_{hw}) \quad (2)$$

where γ_{ho}, γ_{wo}, and γ_{hw} are the hydrogel/oil, water/oil, and hydrogel/water interfacial tensions, respectively. Whether the oil phase facilitates water spreading depends on $\Delta S = S' - S$. If ΔS is larger than 0, then the oil phase can facilitate water spreading on hydrogel surfaces, otherwise the oil phase hinders water spreading. The calculated $\Delta S = 14.1\ \mathrm{mN\,m^{-1}}$ (Supporting Information), indicates improved water spreading. On the other hand, the increase of oil depth can lead to the decrease of water CAs to reach 0°. In normal cases, water molecules in hydrogels are trap-

ped in the 3D cross-linked polymer networks, which can be considered as porous structures. We reasoned that the hydraulic pressure might open the curved interface inside the pores at the hydrogel surfaces.[12] Therefore, the capillary effect induced by the deformation of the pores will enhance the spreading of water droplets. To support this hypothesis, we measured the shear modulus of the hydrogel. Based on the shearing modulus (7.4 kPa; Figure S2), the hydraulic pressure (2.9 kPa, depth: 30 cm) should be high enough to induce the deformation of the hydrogel surfaces, thus leading to the decrease of water CAs.

In addition, the miscibility[13,14] between spreading liquids and liquid phase in the gels is also crucial for superspreading. The perfluoropolyether (PFPE, immiscible with water), ethyl acetate (solubility in water: 7.4 wt%), and methyl ethyl ketone (solubility in water: 27.1 wt%) were chosen as controls. Figure S3 shows that the partially miscible liquids exhibit various spreading states; completely miscible liquids show superspreading. During the spreading process, the simultaneous spreading and interdiffusion can induce the compositional gradients,[14] which can result in surface tension gradients (towards the edge of the spreading liquids), and consequently drive the spreading of liquids on gel surfaces to saturation. In contrast, liquids exhibited partial spreading on the corresponding solid surfaces (Figure S4) and gel surfaces (Figure S5).

Using the water/oil/organogel system as a model, we investigated the spreading behaviors of a series of oils with low viscosity (≈several cSt) on their mutually soluble P(BMA-*co*-LMA) organogel surfaces (Figure S6). As summarized in Table 1, the superspreading of all the miscible oils and liquid monomers was realized on these organogel surfaces (Figure S7). In contrast, partial spreading was observed for miscible oils on solid P(BMA-*co*-LMA) surfaces and immiscible PFPE oil on both solid and organogel surfaces.

Table 1: Superspreading of various low viscous oils on organogel surfaces in a water/oil/organogel system.

Gel \ Spreading oil	Silicone oil	Petroleum ether	Hexane	Chloroform	Toluene	Styrene	Pyrrole	Aniline	PFPE
Petroleum ether-organogel	○	○	○	○	○	○	○	○	x
Hexane-organogel	○	○	○	○	○	○	○	○	x
Chloroform-organogel	○	○	○	○	○	○	○	○	x
Toluene-organogel	○	○	○	○	○	○	○	○	x
Solid P(BMA-*co*-LMA)	x	x	x	x	x	x	x	x	x

○: Superspreading **X**: Partial spreading

The rapid spreading of highly viscous liquids on surfaces is important in a variety of practical processes.[15] In our strategy, the superspreading of high viscosity liquids can be improved by the hydraulic pressure. As their concentrations increased, high viscosity polymer solutions showed a transition from superspreading to partial spreading on the chloroform-swollen P(BMA-*co*-LMA) organogel (hereafter referred to as organogel for short) surfaces under water (Figure S8). Owing to the variety of polymer solubilities in organic solvents, we utilized silicone oils with a series of viscosities ranging from 2000 cSt to 16000 cSt to investigate the spreading behaviors of high viscosity oils on organogel surfaces under water. As shown in Figure 3a, silicone oils with viscosity below the critical transition viscosity (CTV, 6000 cSt at a water depth of 1 cm) showed superspreading on organogel surfaces. Silicone oils whose viscosities were higher than 6000 cSt showed partial spreading on organogel surfaces. The spreading degrees (advancing CA as measurement parameter) decreased with increasing oil viscosity. The observation time was no more than 240 s (Figure S9). We

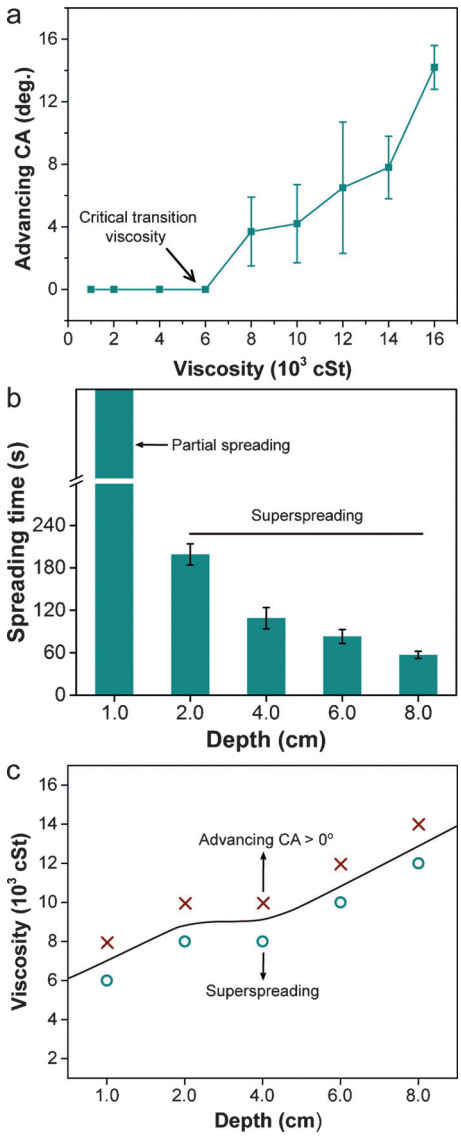

Figure 3. Hydraulic pressure enhances spreading of high viscous silicone oils on organogel surfaces in a water/oil/organogel system. a) Silicone oils with viscosity higher than 6000 cSt showed partial spreading on organogel surfaces under water for a short time (up to 240 s, water depth: 1 cm). b) By increasing the water depth, the oil droplets spread faster. With the aid of hydraulic pressure, the spreading of highly viscous silicone oil can be accelerated. c) The increase of CTV with the aid of hydraulic pressure.

consider the oils capable of complete spreading within 240 s as able to achieve superspreading on organogel surfaces.

It is worth noting that we can convert the partial spreading into superspreading with the assistance of hydraulic pressure. Silicone oil (8000 cSt) was partially spreading on organogel surfaces at the water depth of 1 cm (Figure 3b). After increasing the water depth to 2 cm, the silicone oil could completely spread on organogel surfaces within 199.3 ± 15.1 s. Further increasing the water depth dramatically decreased the spreading time. The silicone oil could completely spread on organogel surfaces within 57.3 ± 5.1 s when the water depth was increased to 8 cm. Furthermore, the partial spreading of a series of high viscosity silicone oils can be enhanced into superspreading with the aid of hydraulic pressure. The CTV is around 6000 cSt when the organogel surfaces at a depth of 1 cm (Figure 3c). Increasing the water depth from 1 cm to 8 cm, the CTV was dramatically promoted from 6000 cSt to 12000 cSt. These results indicate that the introduction of a liquid phase can facilitate the superspreading of high viscosity liquids.

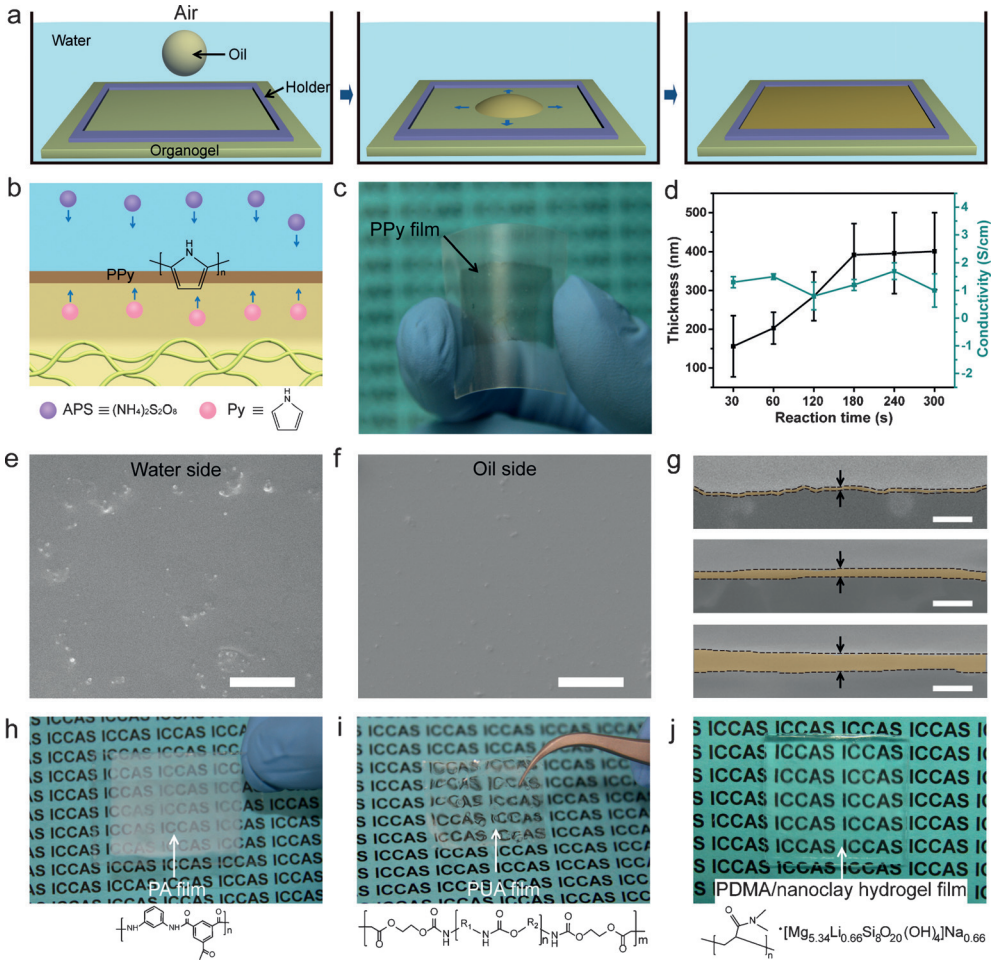

Figure 4. Confined liquid layers for the synthesis of thin polymer films on gel surfaces in a liquid/liquid/gel system. a) The confined superspreading layers of oils with controlled thickness can be realized by using a holder. b) Schematic of the fabrication of thin PPy film at organogel surfaces based on the confined superspreading layers of oils. c) The synthetic thin PPy film trasfferd to flexible substrate. d) Controlled thicknesses of thin PPy films and corresponding conductivities. e–f) SEM images of water side (e) and oil side (f) of the PPy film. Reaction time: 120 s. Scale bar = 100 μm. g) SEM images of PPy films with different thicknesses (yellow colored area, reaction time: top, 30 s; middle, 120 s; bottom, 240 s). Scale bar = 500 nm. h–j) Optical images of the synthetic thin PA film on glass surface (h), free-standing thin PUA film (i), and free-standing PDMA/nanoclay composite hydrogel film (j).

By using an on-demand holder, we can control the liquid spreading and obtain a confined, stable, and homogeneous liquid layer on gel surfaces (Figures 4a and S10).

By introducing the reactants into the superspreading liquid layers, various functional thin polymer films, whose thickness can be controlled from several hundreds of micrometers to tens of nanometers, can be fabricated through a one-step polymerization reaction. For example, we successfully synthesized conducting thin polypyrrole (PPy) films with controlled thicknesses at the nanometer scale. Traditional methods to fabricate PPy films are based on water/oil interfacial polymerization.[16] However, the processability remains a challenging issue because the water/oil interfaces formed in the bulk liquid phases can be easily disturbed by external interference, which hamper the continuous fabrication of PPy films.[17] This issue could be effectively settled by our superspreading strategy. Since the fluidity of the confined oil layer was restricted by the organogels, the stability of the spreading liquid layer was significantly improved. The oxidant and monomer were introduced to the water phase and oil layers, respectively (Figure 4b). After redox polymerization, thin PPy films were formed at the organogel surfaces. Owing to the liquid-like property of the organogel surfaces, the formed films could be readily separated from the organogel surface and transferred to many kinds of material surfaces (Figures 4c and S11–S12). Furthermore, by regulating the reaction time, the thickness of the thin PPy films can be controlled from 150–400 nm, while the conductivities of these PPy films can be kept around 1 S cm (Figures 4d,g and S13). The SEM images show that the fabricated PPy films have smooth and uniform surfaces (Figures 4e,f and S14).

Based on the confined oil layers, we can also conduct a series of chemical reactions for one-step synthesis of free-standing thin polymer films with controlled thicknessesw.

Traditional interfacial polymerization for the fabrication of thin polyamide (PA) films suffers from several shortcomings, including multiple steps, uneven surfaces, and limited areas.[5a,16,18] Here, we synthesized thin PA films with smooth surfaces and controlled thicknesses by using our superspreading strategy (Figures 4h and S15–S16). The *m*-phenylenediamine (MPD) and trimesoyl chloride (TMC) reagents were dissolved in water and spreading oil separately. Thin PA films, whose thicknesses could be tuned from 500 to 1200 nm by controlling the reaction time, were successfully fabricated at the organogel surface. We also fabricated free-standing poly(urethane acrylate) (PUA) films[19] with one-step photo-polymerization of its oligomer. The oligomer and photo-initiator were simultaneously introduced in the confined superspreading oil layers. A free-standing and transparent thin PUA film with smooth surface was formed after irradiating with UV light for 2 min (Figures 4i; and S17). The thickness of the resulting PUA films ranged from 30 to 140 μm, and could be easily manipulated by regulating the volumes of spreading oils (Figure S18).

Except for the polymerization in water/oil/organogel systems, the superspreading in oil/water/hydrogel systems can be also used for the one-step synthesis of polymer films with defined thicknesses. For instance, we could prepare polydimethylacrylamide (PDMA)/nanoclay composite hydrogel films with excellent tensile properties by regulating the content of nanoclay, even under highly viscous conditions (Figures 4j and S18).

In summary, we demonstrated that the superspreading of liquids on their mutually soluble gel surfaces can be utilized to fabricate various functional thin polymer films. Owing to the hydraulic pressure and liquid-like property of gel surfaces, the stable and homogeneous superspreading layers of liquids can be achieved. Furthermore, such liquid layers can be converted into various functional thin polymer films, including PPy, PA, PUA, and PDMA/nanoclay composite hydrogel films with various thicknesses through a one-step polymerization reaction. Our strategy offers opportunities to fabricate functional thin polymer films for various applications. Future perspectives may include the design of appropriate equipment for continuous and large-scale fabrication of polymer thin films (Figure S19). This work can encourage the development of conceptually novel superwettability-based chemistry and fabrication.

Acknowledgements

This research is supported by the National Natural Science Foundation (21574004, 21422061), National Research Fund for Fundamental Key Projects (2013CB933000, 2012CB933800, 2012CB934100, and 2014CB932203), the Key Research Program of the Chinese Academy of Sciences (KJZD-EW-M01, KJZD-EW-M03), and the 111 project (B14009).

Keywords: hydrogels · organogels · superspreading · thin polymer films · under-liquid

How to cite: *Angew. Chem. Int. Ed.* **2016**, *55*, 3615–3619
Angew. Chem. **2016**, *128*, 3679–3683

[1] P. G. de Gennes, *Rev. Mod. Phys.* **1985**, *57*, 827–863.
[2] a) L. Courbin, E. Denieul, E. Dressaire, M. Roper, A. Ajdari, H. A. Stone, *Nat. Mater.* **2007**, *6*, 661–664; b) G. McHale, N. J. Shirtcliffe, S. Aqil, C. C. Perry, M. I. Newton, *Phys. Rev. Lett.* **2004**, *93*, 036102; c) J. Bico, C. Tordeux, D. Quéré, *Europhys. Lett.* **2001**, *55*, 214.
[3] a) K. P. Ananthapadmanabhan, E. D. Goddard, P. Chandar, *Colloids Surf.* **1990**, *44*, 281–297; b) J. Venzmer, *Curr. Opin. Colloid Interface Sci.* **2011**, *16*, 335–343; c) T. Stoebe, Z. Lin, R. M. Hill, M. D. Ward, H. T. Davis, *Langmuir* **1996**, *12*, 337–344.
[4] a) A. G. Emslie, F. T. Bonner, L. G. Peck, *J. AppL. Phys.* **1958**, *29*, 858–862; b) Y. Yuan, G. Giri, A. L. Ayzner, A. P. Zoombelt, S. C. B. Mannsfeld, J. Chen, D. Nordlund, M. F. Toney, J. Huang, Z. Bao, *Nat. Commun.* **2014**, *5*, 3005.
[5] a) M. A. Shannon, P. W. Bohn, M. Elimelech, J. G. Georgiadis, B. J. Marinas, A. M. Mayes, *Nature* **2008**, *452*, 301–310; b) S. R. Forrest, *Nature* **2004**, *428*, 911–918; c) X.-L. Liu, Y.-S. Li, G.-Q. Zhu, Y.-J. Ban, L.-Y. Xu, W.-S. Yang, *Angew. Chem. Int. Ed.* **2011**, *50*, 10636–10639; *Angew. Chem.* **2011**, *123*, 10824–10827; d) A. G. Fane, R. Wang, M. X. Hu, *Angew. Chem. Int. Ed.* **2015**, *54*, 3368–3386; *Angew. Chem.* **2015**, *127*, 3427–3447.
[6] a) F. Heslot, N. Fraysse, A. M. Cazabat, *Nature* **1989**, *338*, 640–642; b) M. N. Popescu, G. Oshanin, S. Dietrich, A. M. Cazabat, *J. Phys. Condens. Matter* **2012**, *24*, 243102.
[7] D. Bonn, J. Eggers, J. Indekeu, J. Meunier, E. Rolley, *Rev. Mod. Phys.* **2009**, *81*, 739–805.
[8] a) M. S. Jhon, J. D. Andrade, *J. Biomed. Mater. Res.* **1973**, *7*, 509–522; b) Y. Osada, J.-P. Gong, *Adv. Mater.* **1998**, *10*, 827–837.
[9] a) F. J. Holly, M. F. Refojo, *J. Biomed. Mater. Res.* **1975**, *9*, 315–326; b) M. Banaha, A. Daerr, L. Limat, *Eur. Phys. J. Spec. Top.* **2009**, *166*, 185–188; c) H. Frank J, R. Miguel F, in *Hydrogels for Medical and Related Applications*, *Vol. 31*, American Chemical Society, Washington, DC, **1976**, pp. 252–266.
[10] a) H. Liu, P. Zhang, M. Liu, S. Wang, L. Jiang, *Adv. Mater.* **2013**, *25*, 4477–4481; b) P. Zhang, H. Liu, J. Meng, G. Yang, X. Liu, S. Wang, L. Jiang, *Adv. Mater.* **2014**, *26*, 3131–3135; c) X. Yao, S. S. Dunn, P. Kim, M. Duffy, J. Alvarenga, J. Aizenberg, *Angew. Chem. Int. Ed.* **2014**, *53*, 4418–4422; *Angew. Chem.* **2014**, *126*, 4507–4511; d) X. Yao, S. Wu, L. Chen, J. Ju, Z. Gu, M. Liu, J. Wang, L. Jiang, *Angew. Chem. Int. Ed.* **2015**, *54*, 8975–8979; *Angew. Chem.* **2015**, *127*, 9103–9107.
[11] W. D. Harkins, A. Feldman, *J. Am. Chem. Soc.* **1922**, *44*, 2665–2685.
[12] a) J. R. Rice, M. P. Cleary, *Rev. Geophys.* **1976**, *14*, 227–241; b) G. W. Scherer, D. M. Smith, *J. Non-Cryst. Solids* **1995**, *189*, 197–211; c) X. Yao, Y. Hu, A. Grinthal, T.-S. Wong, L. Mahadevan, J. Aizenberg, *Nat. Mater.* **2013**, *12*, 529–534.
[13] E. Saiz, A. P. Tomsia, *Nat. Mater.* **2004**, *3*, 903–909.
[14] P. G. De Gennes, *Macromolecules* **1986**, *19*, 1245–1249.
[15] a) L. H. Tanner, *J. Phys. D* **1979**, *12*, 1473–1484; b) C. W. Extrand, *J. Colloid Interface Sci.* **1993**, *157*, 72–76.
[16] P. W. Morgan, S. L. Kwolek, *J. Polym Sci.* **1959**, *40*, 299–327.
[17] a) U. Sree, Y. Yamamoto, B. Deore, H. Shiigi, T. Nagaoka, *Synth. Met.* **2002**, *131*, 161–165; b) G. Qi, Z. Wu, H. Wang, *J. Mater. Chem. C* **2013**, *1*, 7102–7110.
[18] W. Xie, G. M. Geise, B. D. Freeman, H.-S. Lee, G. Byun, J. E. McGrath, *J. Membr. Sci.* **2012**, *403–404*, 152–161.
[19] H. Xu, F. Qiu, Y. Wang, W. Wu, D. Yang, Q. Guo, *Prog. Org. Coat.* **2012**, *73*, 47–53.

Received: November 5, 2015
Revised: January 20, 2016
Published online: February 15, 2016

